SRTTU

JCARME
ISSN: 2228-7922
Journal of Computational and Applied Research in Mechanical Engineering
Vol. 9, No. 2, pp. 397-407
jcarme.sru.ac.ir

Development length of laminar magnetohydrodynamics pipe flows

Mohammad Hasan Taheri*, Morteza Abbasi and Mehran Khaki Jamei

Department of Mechanical Engineering, Sari Branch, Islamic Azad University, Sari, Iran

Article info:

Received: 22/11/2018
Revised: 29/01/2019
Accepted: 03/02/2019
Online: 05/02/2019

Keywords:
Artificial neural networks,
Development length,
Finite volume method,
Magnetohydrodynamics,
Pipe.

Abstract

In this article, a laminar magnetohydrodynamics (MHD) developing flow of an incompressible electrically conducting fluid subjected to an external magnetic field is considered. The aim of the study is to propose a correlation for computing the development length of the laminar MHD developing flow in a pipe. A numerical approach is considered to solve the problem. In the first step, the numerical Finite Volume Method (FVM) is conducted to analyze the problem. Hereafter, the artificial neural network (ANN) is used to develop the datasets and in the last step, the curve fitting is applied to find a correlation for the prediction of the development length as a function of the Reynolds and Hartmann numbers. In addition, the effect of the problem parameters on the development length is studied. It is found that the development length declines with the increase of the Hartmann number and grows with the rising of the Reynolds number.

Nomenclature

B	Total magnetic field (T)
B_0	External magnetic field (T)
b	Induced magnetic field (T)
E	Electric field (N/C)
F_L	Lorentz force (N)
Ha	Hartmann number
J	Density of electric current (A/m^2)
ℓ	Characteristic length (m)
L_{em}	MHD development length (m)
σ	Electrical conductivity $(\Omega.m)^{-1}$
P	Gauge pressure (Pa)
r	Radius of the pipe (m)
Re	Reynolds number
u_{av}	Mean velocity (m/s)
u_r	r- component of the velocity (m/s)
u_z	z- component of the velocity (m/s)
$(u_z)_c$	centerline velocity (m/s)
$(u_z)_{cm}$	MHD centerline velocity (m/s)
$(u_z)_{cmf}$	MHD fully developed centerline velocity (m/s)
$\vec{V}$	Velocity field (m/s)
z	Coordinate in the direction of flow (m)
ρ	Density (kg/m^3)
μ	Dynamic viscosity ($Pa.s$)
∇	Del operator

1. Introduction

Precise prediction of the development length for MHD pipe flow is a significant subject in several fields. Examples in engineering applications include design and analysis of pipe flow systems, MHD wind tunnels and flow instrumentations like MHD flowmeters and MHD viscometers, industrial applications

* *Corresponding author*
email address: hasan.taheri@gmail.com

involving metallurgical processing, MHD pumps, piping systems in reactors and the physiological applications like the MHD blood flow simulation in vascular networks [1-6].

Although much research has been done to find a correlation for predicting the hydrodynamic development length in the pipes [7-14], there is little research on computing the MHD development length. According to the available literature, some experimental [15, 16], analytical [17-19] and numerical investigations [20-22] have been carried out on the MHD developing flow in circular and non-circular channels. In these studies, a two- or three-dimensional MHD pipe flow subjected to a uniform or non-uniform external magnetic field was studied and the velocity profile, the pressure loss and other flow characteristics were investigated.

He and Ku [23] investigated the unsteady entrance flow in pipes numerically and evaluated the development length variations of a pulsatile flow due to its importance in some blood flow situations. Li et al. [24] studied the MHD two-phase (liquid metal-gas) flow in an annular channel numerically and reported at the same conditions of the liquid phase flow that the pressure loss has a similar order of magnitude to the one in the single-phase MHD pipe flow. Durst et al. [25] reviewed the correlations proposed for computing the development length for non-MHD pipe flows available in the literature until then. They studied a laminar developing pipe flow using numerical finite volume method and proposed a correlation for estimating the entrance length of the laminar pipe flows without MHD effects. In the same way, Pool and Ridley [14] presented the summary of the entry length correlations for non-MHD pipe flows of the non-Newtonian power-law fluids, and offered a new formula for calculating the development length as a function of the power-law index and the modified Reynolds number.

Malekzadeh et al. [26] carried out an experimental and numerical study on the magnetic field effect for laminar fully developed pipe flows characteristics. They examined the flow field for four Reynolds numbers (1000,1500 and 2000) and seven Hartmann numbers (0, 2.5, 5, 7.5, 10, 12.5 and 15) and offered an approximate numerical expression for computing the entrance length of MHD pipe flow. Sahu et al. [11] presented a numerical based model named ANFIS (adaptive network fuzzy inference system) to predict the development length of the low Reynolds number pipe flow (Re<500) without MHD effects. The results were found in good agreement with the earlier works. Ray et al. [12] explored the laminar fully developed pulsating pipe flows numerically and proposed a correlation to predict the maximum entrance length of non-MHD pipe flows during a cycle, for the moderate and high Reynolds number regimes.

Li and Zikanov [27] investigated the laminar MHD pipe flows numerically and discussed the structure of the flow with an M-shaped velocity profile. Moreover, they established the criteria, which could be used to study the laminar MHD pipe flows under the strong non-uniform magnetic fields. Li et al. [28] studied the pressure drop of a three-dimensional liquid metal pipe flow under the effect of a non-uniform magnetic field. They reported the experimental results of the pressure distribution patterns and concluded that the 3D numerical simulations led to appropriate results that were in good agreement with the empirical data.

Ray et al. [9] investigated the velocity profile development and the pressure drops of the micro-pipe entrance flow with second-order slip boundary conditions and offered a correlation to compute the entrance length of the non-MHD micro-pipe flows. Patel [10] studied the effect of an external uniform magnetic field on the velocity profile of a steady state MHD pipe flow using numerical finite difference scheme. They showed the flattening of the axial velocity profile due to the presence of the magnetic field graphically and discussed about the increase of the friction factor.

Bühler and Mistrangelo [29] numerically explored the pressure drop and the velocity profile variations in MHD pipe flow as a result of a local gap of the walls insulation. They concluded that although the existence of the interruptions in pipe insulation might result in the lower pressure losses, it could cause the undesirable effects on the velocity profile and thus the heat and mass transfer phenomena.

Okita et al. [2] carried out an experimental investigation to study the liquid metal MHD flow and measure the mean velocity of the flow by an Electro-Magnetic Flowmeter (EMF) and presented the velocity profiles for the two special cases of the magnetic flux density.
The literature survey reveals that although the subjects of the MHD channel and pipe flows were widely investigated [30-35] and the correlations for computing the development length of the non-MHD pipe flows were reported for several cases and different applications, but a reliable correlation for computing the development length of the MHD pipe flows is not available. Hence, the motivation of the present study is proposing a correlation for computing the development length of the laminar two-dimensional MHD pipe at the entrance region. The numerical finite volume method is applied to solve the problem. Then, using ANN the data is developed and finally, the curve fitting is treated to find the correlation. In addition, the effects of different parameters on the MHD development length, the MHD fully developed centerline velocity and the Lorentz force are evaluated.

2. Problem statement

The schematic configuration of the problem is shown in Fig. 1. A steady laminar liquid metal flow through a pipe with the no-slip boundary condition on the walls is considered. A liquid metal flow with a uniform velocity distribution enters the pipe. After passing the specified length of the pipe (z_0), called the hydrodynamic entrance length, the development of the flow is completed and the velocity profile gets a parabolic form (i.e. the hydrodynamically fully developed velocity profile of the pipe flows).
From that section, a uniform transverse magnetic field (B_0) is imposed on the pipe flow, perpendicularly, so that the parabolic velocity profile converts into a new form gradually, which is the MHD fully developed velocity profile of the MHD pipe flows. The development length is defined as the distance from inlet; the magnitude of the centerline velocity reaches to 99 percent of the fully developed velocity magnitude. The considered MHD pipe has a length of $0.7m$ and a radius of $0.005m$.

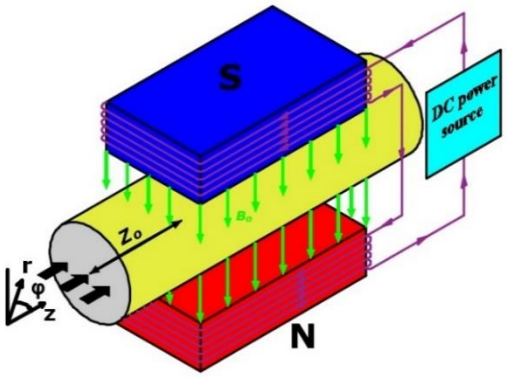

Fig. 1. Problem schematic.

3. Mathematical model

The governing equations of the described problem including continuity, momentum and Ohm's law are introduced as follows:

$$\nabla.\vec{V} = 0 \tag{1a}$$

$$\rho\left(\vec{V}.\nabla\right)\vec{V} = -\nabla\vec{P} + \mu\nabla^2\vec{V} + \sigma\left(\vec{J}\times\vec{B}\right) \tag{1b}$$

$$\vec{J} = \sigma\left(\vec{E} + \vec{V}\times\vec{B}\right) \tag{1c}$$

Whereas V, P, J, E and B are the velocity field, the gauge pressure, the electric current density, the electrical field and the total magnetic field (i.e. the sum of the external magnetic field (B_0) and the induced magnetic field (b)), respectively. The fluid properties are assumed constant and the effect of the body forces is negligible except for the Lorentz body force, given as follows [36]:

$$\vec{F}_L = \vec{J}\times\vec{B} = \sigma\left(\vec{E} + \vec{V}\times\vec{B}\right)\times\vec{B} \tag{2}$$

In the absence of the electric field and while the magnetic Reynolds number is small enough, the induced magnetic field can be ignored and the Lorentz force is simplified as:

$$\vec{J}\times\vec{B} = -\sigma B_0^2 u_z\,\hat{e}_z \tag{3}$$

According to the described assumptions, Eqs. (1) can be rewritten as:

$$\frac{1}{r}\frac{\partial}{\partial r}(\rho r u_r)+\frac{\partial}{\partial z}(\rho u_z)=0 \quad (4a)$$

$$\rho\left(u_r\frac{\partial u_z}{\partial r}+u_z\frac{\partial u_z}{\partial z}\right)= -\frac{\partial P}{\partial z}+\mu\left[\frac{1}{r}\frac{\partial}{\partial r}\left(r\frac{\partial u_z}{\partial r}\right)+\frac{\partial^2 u_z}{\partial z^2}\right]-\sigma B_0^2 u_z \quad (4b)$$

$$\rho\left(u_r\frac{\partial u_r}{\partial r}+u_z\frac{\partial u_r}{\partial z}\right)= -\frac{\partial P}{\partial r}+\mu\left[\frac{\partial}{\partial r}\left(\frac{1}{r}\frac{\partial}{\partial r}(r u_r)\right)+\frac{\partial^2 u_r}{\partial z^2}\right] \quad (4c)$$

The boundary conditions of the defined problem are introduced as:

$$z=z_0 \quad \rightarrow u_z=(u_z)_c\left[1-\left(\frac{r}{0.005}\right)^2\right], u_r=0 \quad (5a)$$

$$r=0.005 \rightarrow \quad u_r=u_z=0 \quad (5b)$$

$$z=z_0+0.7 \quad \rightarrow \quad P=0 \quad (5c)$$

Where $(u_z)_c$ is the centerline velocity.

Two dimensionless parameters are important for computing the MHD development length, the Reynolds (Re) and the Hartmann (Ha) numbers are defined as follows:

$$\mathrm{Re}=\frac{\rho u_{av}\ell}{\mu} \quad (6a)$$

$$Ha=B\ell\sqrt{\frac{\sigma}{\mu}} \quad (6b)$$

Where ℓ is the characteristic length. In the present study, the pipe radius (r) is the characteristic length. The mean velocity (u_{av}) is defined as:

$$u_{av}=\frac{\int_A \rho V.\hat{n}\,dA}{\rho A}=\frac{1}{2}(u_z)_c \quad (7)$$

4. Solution method

In the first step, the numerical finite volume method (FVM) is employed to solve the governing Eqs. (4a, b, c) in order to obtain a reliable correlation for predicting the development length of pipe flows. Central differencing is used for the diffusive terms, while the second-order upwind scheme is applied for the convective terms. In order to avoid round-off errors, double precision is used for all calculations. The SIMPLE algorithm is employed for the pressure-velocity coupling and the momentum and continuity equations are solved using the steady-state iterative algorithm. Furthermore, to have the converged results, the residual error is selected 10^{-5}.

The results of the mesh independence are present in Table 1 and Fig. 2. It should be noted that the heavy liquid metal Lead–Bismuth (Pb-Bi) was selected in this study, due to its application as a coolant for the new generation reactors [37-39]. Applying Pb-Bi physical properties [40], the numerical procedure is performed for the Reynolds number ranging from 700 to 1180 while the Hartman number varied from 7 to 14. For each range, the development length value of the pipe is calculated. Therefore, 72 datasets are reached.

In the second step, the ANN is conducted. The main goal of using ANN is to accelerate the procedure of numerical solving especially for the complex problems that have a long time CPU time. In order to use ANN, 72 datasets obtained in the first step are used to train in a feed-forward back-propagation network. In this network, the Reynolds and Hartmann number are considered as an input data and the development length is considered as a target data. Levenberg-Marquardt (LM) algorithm is used to determine the appropriate multi-layer functions for describing the relationship between inputs and target data. The appropriate network can be reached when the mean square error between the output data and the target is minimized. As the error becomes constant, the train process is stopped (Fig. 3). Finally, the trained network with determined accuracy will be reached.

Table 1. Results of mesh independence study for $(u_z)_{cmf}$ (Ha = 10, Re = 810).

Mesh size (mm)	$(u_z)_{cmf}$ (m/s)
0.9	0.0436
0.6	0.0433
0.4	0.0432

0.3	0.0432

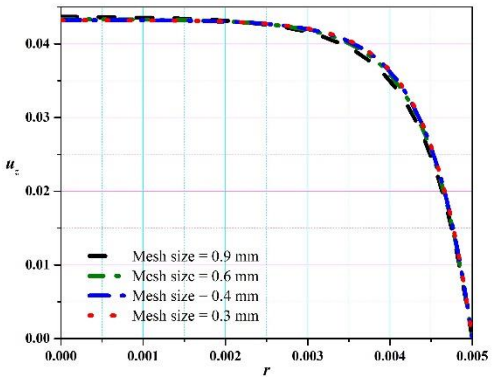

Fig. 2. Results of mesh independence study for $(u_z)_{cmf}$ (Ha = 10, Re = 810).

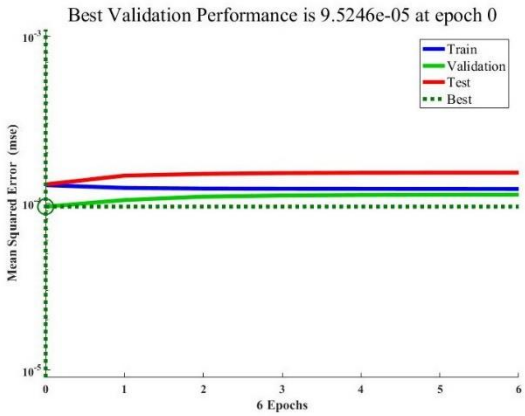

Fig. 3. Neural network training performance.

In Table 2, the characteristic of the trained network, the neuron and layer numbers are reported. Therefore, using trained ANN, 308 datasets are obtained for the Re range from 500 to 2000 while Ha varied from 4 to 20. Now in the last step, all 308 datasets are used to fit a curve and the correlation will be obtained.

5. The proposed correlations

Considering the mentioned steps, the proposed correlations for predicting the development length as a function of the Reynolds and the Hartmann numbers are defined as following:

$$\begin{aligned} &for \quad (750 \le \mathrm{Re} < 1100,\ 5 \le Ha \le 18) \\ &and \quad (1100 \le \mathrm{Re} \le 2000,\ 5 \le Ha \le 19): \end{aligned} \tag{8a}$$

$$\begin{aligned} L_{em} = {} & 153.82 + Ha\left[(-0.6684 + 0.04974Ha)Ha\right] \\ & + Ha\left[0.019438\,\mathrm{Re} - 16.45\right] \\ & + \mathrm{Re}\left[(-8.036\times10^{-4}\,Ha + 5.816\times10^{-7}\,\mathrm{Re})Ha\right] \\ & + \mathrm{Re}\left[-2.92\times10^{-5}\,\mathrm{Re} + 0.026\right] \end{aligned}$$

$$\begin{aligned} &for \quad (650 \le \mathrm{Re} \le 1400,\ 7 \le Ha \le 15) \\ &and \quad (1400 \le \mathrm{Re} \le 1800,\ 9 \le Ha \le 20) \end{aligned} \tag{8b}$$

$$\begin{aligned} L_{em} = {} & -18.944 + Ha\left[(-1.1288\times10^{-6}\,\mathrm{Re}^2 - 4.618\times10^{-3}\,Ha^2)\,Ha\right] \\ & + Ha\left[(1.0252\times10^{-4}\,\mathrm{Re}\,Ha + 0.18408\,Ha - 2.284)\,Ha + 6.01\right] \\ & + \mathrm{Re}\left[(-2.372\times10^{-3}\,Ha + 3.42\times10^{-5}\,\mathrm{Re} - 3.944\times10^{-3})\,Ha\right] \\ & + \mathrm{Re}\left[-2.684\times10^{-4}\,\mathrm{Re} + 0.3522\right] \end{aligned}$$

Where L_{em} is the MHD development length.

6. Validation checking of the proposed correlations

In order to validate the proposed formulas (Eqs. 8), the available proven results in the literature were applied.

Table 3 shows the comparison between the results of the proposed correlations (8 a and b) and the available literature data. As can be seen, the results obtained from our presented formulas are in good agreement with the validated data.

Moreover, in Table 4 the values of the development length obtained from three different methods are presented. It can be seen that there is reasonable agreement among the development length values of these three different methods and ANN can be used to model and predict the MHD flow and development length.

Table 2. Characteristics of the trained network.

Layers number	Training function	Neurons number	Ha range	Re range
2	1st layer: Log-sigmoid	1st layer: 2	7-14	700 – 1180
	2nd layer: Pure line	2nd layer:1		

Table 3. Validation of the proposed correlations.

	Re	Ha	Ref result	Eq. (8)
Durst et al. [25]	800	0	0.228	0.227

Mohanty &Asthana [41]	1000	0	0.375	0.377
	700	20	0.058	0.053
Malekzadeh et al. [26]	1450	4	0.500	0.520
	1700	5	0.510	0.500

Table 4. The comparison of the magnetic development length among three methods.

				L_{em}	
Re	Ha	FVM	ANN	Eq. (8a)	Eq. (8b)
700	9	0.360	0.365	0.356	0.340
880	10	0.382	0.376	0.3836	0.3847
1000	14	0.245	0.242	0.242	0.238
1180	7	0.667	0.669	0.666	0.663
1240	7	0.684	0.680	0.682	0.677
1300	7	0.688	0.6902	0.7	0.686
1360	7	0.692	0.6982	0.7	0.686
1480	8	0.696	0.6974	0.718	0.695
1540	9	0.685	0.6883	0.701	0.687
1600	9	0.695	0.696	0.719	0.698
1660	10	0.688	0.6873	0.701	0.69

7. Results and discussion

The effect of Hartmann number on the entrance length is depicted in Fig. 4. As can be seen, by increasing *Ha*, the development length decreases. *Ha* is the ratio of the Lorentz forces to the viscous forces. According to Eq. (3), the Lorentz force is a resistance force, proportional to the velocity. Indeed, augmentation of the Lorentz force causes velocity reduction in the potential region above the boundary layer. Eventually, the development length decreases.

Figs. 5 and 6 represent the development of the MHD centerline velocity (u_{cm}) in the flow direction, for different values of the Hartmann and the Reynolds numbers, respectively. It is observed that the MHD centerline velocity decreases as Ha increases.

However, as Re increases, the MHD centerline velocity increases. Moreover, as can be seen with the augmentation of the Hartmann number and the reduction of the Reynolds number, the MHD entry length gets shorter.

The velocity vectors (u_z) in the flow direction and for different values of the Hartmann number are demonstrated in Figs. 7. It can be seen that as the Hartmann number rises, the velocity profile at the same cross-section of the pipe becomes flattened.

Similarly, Figs. 8 show the variations of the Lorentz force (F_L) vectors for the different values of the Hartmann number in the flow direction. As discussed later, the Lorentz force is proportional to the velocity field; thus the variation pattern of F_L in the flow direction is similar to u_z changes. However, F_L is a resistance body force, which affects the opposite direction of the flow and velocity vectors.

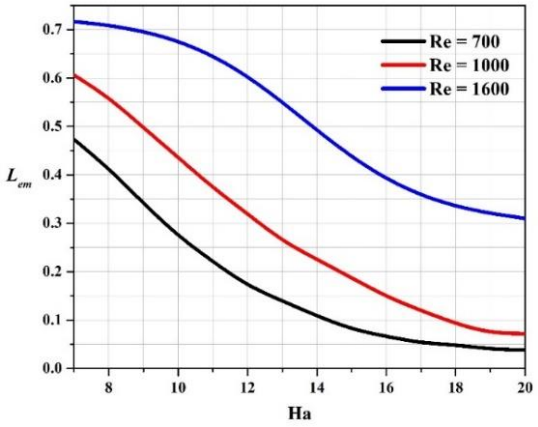

Fig. 4. Effect of Ha on the development length.

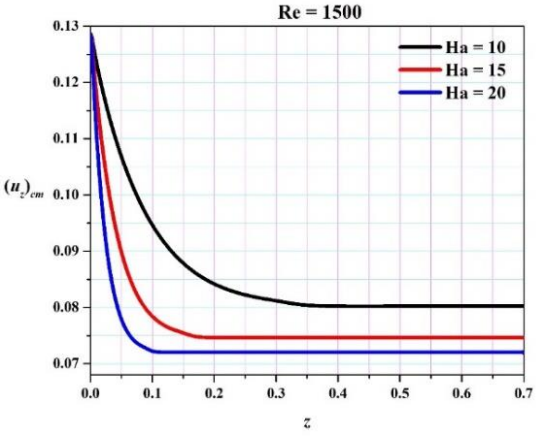

Fig. 5. Effect of Ha on MHD centerline velocity along the pipe length.

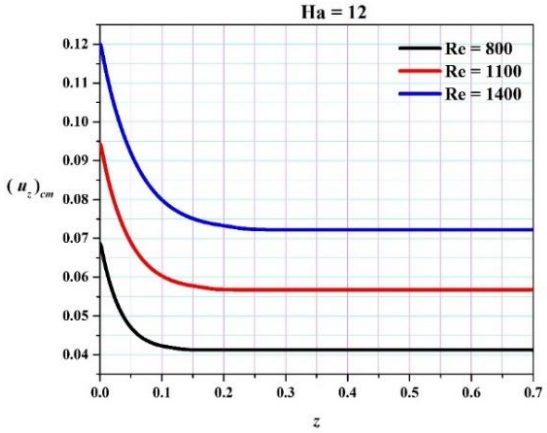

Fig. 6. Effect of Re on MHD centerline velocity along the pipe length.

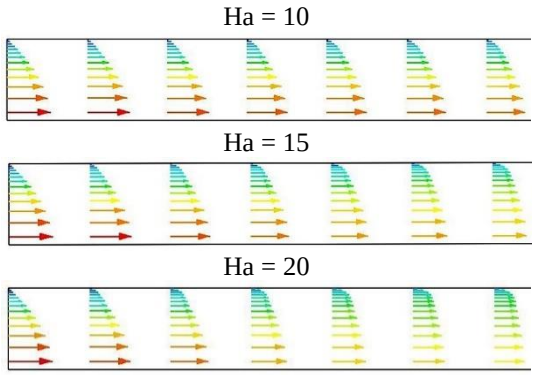

Fig. 7. Axial velocity (u_z) vectors in the flow direction.

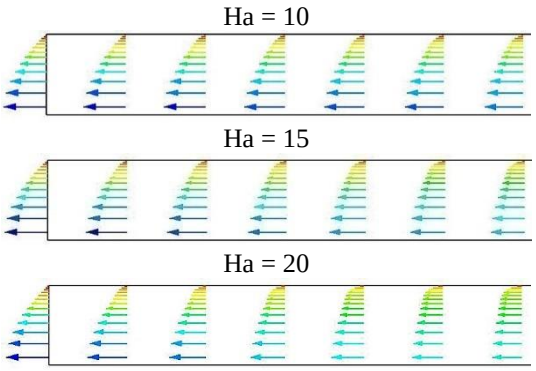

Fig. 8. Lorentz force (F_L) vectors in the flow direction.

Moreover, the velocity profile has the maximum magnitude at the centerline of the pipe; thus the F_L is also maximum at the centerline of the pipe. Also, near the walls, F_L decreases because the velocity magnitude reduces. It can be justified by the fact that as the Reynolds number declines, the thickness of the boundary layers grows and as a result, the MHD development length decreases. On the other hand, while the Hartmann number augments, the resistance Lorentz force (F_L) and the boundary layer growth rise, therefore, the magnetic development length becomes shorter.

The variations of the velocity profile versus *Ha*, along with the r-axis, for the specified value of the Reynolds number are illustrated in Fig. 9. As expected, when *Ha* increases, the velocity profile gets flatten at the same axial position and the fully developed velocity profile arises sooner. This happens because, with augmentation of *Ha*, the Lorentz force, which is the resistance body force and applies in the opposite direction of the flow, increases.

The effect of the Hartmann number on the Lorentz force (F_L) at the MHD pipe centerline is presented in Fig. 10. The Hartmann number is proportional to the Lorentz force, and with increasing *Ha*, F_L increases. In addition, the variation of the Lorentz force (F_L) over the entrance region of the MHD pipe flow can be observed in Fig. 10. It can be seen that, at the pipe centerline, F_L decreases in the flow direction along the channel length at the entry region and when the flow is fully developed, F_L becomes constant.

The variation of the MHD fully developed centerline velocity with respect to Re and *Ha* is plotted in Fig. 11.

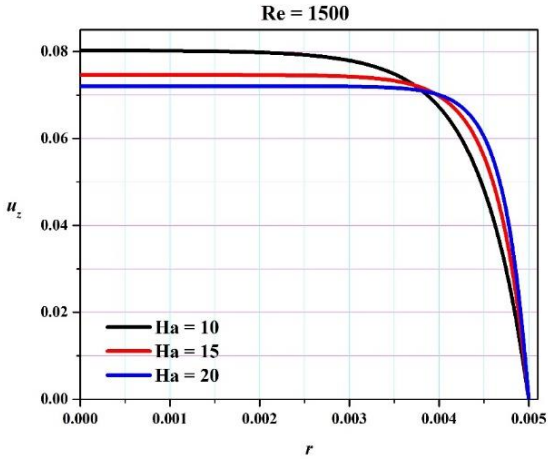

Fig. 9. Velocity profiles for different Ha along the r-axis.

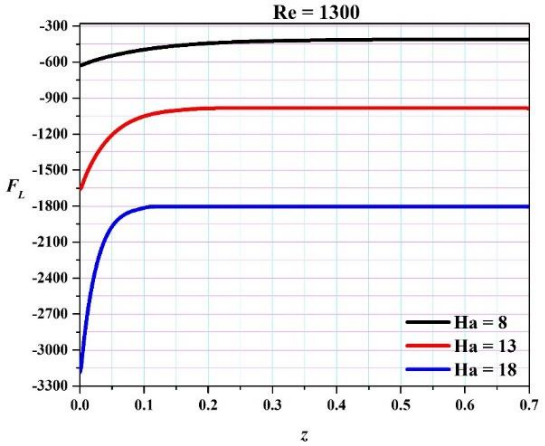

Fig. 10. Effect of Ha on the Lorentz force (F_L).

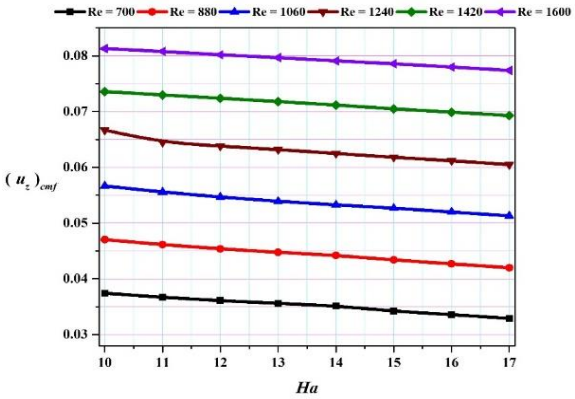

Fig. 11. Effect of Re and Ha on MHD fully developed centerline velocity.

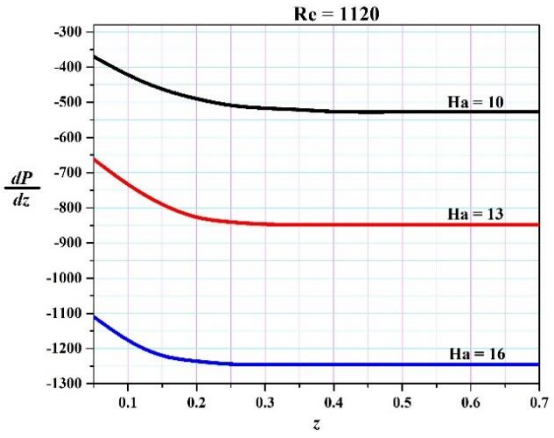

Fig. 12. Effect of Ha on pressure loss.

It can be observed that when *Ha* increases, the magnitude of $(u_z)_{cmf}$ declines. In contrast, augmentation of Re increases the magnitude of $(u_z)_{cmf}$.

In Fig. 12, the changes of the pressure gradient along the pipe length with *Ha* are plotted. It can be seen that as *Ha* increases, the pressure losses grow. Owing to *Ha* that is corresponded with F_L, increasing Ha leads to an increase of the resistance Lorentz force, and consequently the total pressure losses increase.

5. Conclusions

The numerical approach based on finite volume method was applied to solve the steady laminar magnetohydrodynamics pipe flows in the entrance region. A two-dimensional liquid metal developing flow through a pipe subjected to an external magnetic field was studied for different values of the Reynolds and Hartmann numbers. Afterward, the artificial neural network was trained to develop the output datasets obtained from the numerical solution. Eventually, by using the curve fitting on the developed datasets, the correlation for predicting development length was proposed for different ranges of Re and *Ha*. In addition, the effect of Re and *Ha* on the MHD development length, MHD fully developed centerline velocity, pressure losses and the Lorentz force were discussed. It was concluded that with increasing of the Reynolds number, the MHD development length and the MHD fully developed centerline velocity augment; in contrast, the MHD development length and the MHD fully developed centerline velocity reduce when the Hartmann number increases. Furthermore, the results show that with the increase of the Hartmann number the pressure losses rise up.

References

[1] T. J. Rhodes, S. Smolentsev, and M. Abdou, "Effect of the length of the poloidal ducts on flow balancing in a liquid metal blanket," *Fusion Engineering and Design*, Vol. 36, pp. 847-851, (2018).

[2] T. Okita, S. Matsuda, N. Yamaoka, E. Hoashi, T. Yokomine, and T. Muroga, "Study on measurement of the flow velocity of liquid lithium jet using MHD effect for IFMIF," *Fusion Engineering*

and Design, Vol. 136, pp. 178-182, (2018).

[3] A. Javadzadegan, A. Moshfegh, H. H. Afrouzi, and M. Omidi, "Magnetohydrodynamic blood flow in patients with coronary artery disease," *Computer Methods and Programs in Biomedicine*, Vol. 163, pp. 111-122, (2018).

[4] S. Rashidi, J. A. Esfahani, and M. Maskaniyan, "Applications of magnetohydrodynamics in biological systems-a review on the numerical studies," *Journal of Magnetism and Magnetic Materials*, Vol. 439, No. 1, pp. 358-372, (2017).

[5] O. M. Al-Habahbeh, M. Al-Saqqa, M. Safi, and T. Abo Khater, "Review of magnetohydrodynamic pump applications," *Alexandria Engineering Journal*, Vol. 55, No. 2, pp. 1347-1358, (2016).

[6] S.-J. Xu, N.-M. Zhang, and M.-J. Ni, "Influence of flow channel insert with pressure equalization opening on MHD flows in a rectangular duct," *Fusion Engineering and Design*, Vol. 88, No. 5, pp. 271-275, (2013).

[7] Y. Joshi and B. R. Vinoth, "Entry lengths of laminar pipe and channel flows," *Journal of Fluids Engineering*, Vol. 140, No. 6, pp. 061203-061203-8, (2018).

[8] C. Fernandes, L. L. Ferrás, M. S. Araujo, and J. M. Nóbrega, "Development length in planar channel flows of inelastic non-Newtonian fluids," *Journal of Non-Newtonian Fluid Mechanics*, Vol. 255, pp. 13-18, (2018).

[9] B. Ray, F. Durst, and S. Ray, "Pressure drop and flow development in the entrance region of micro-channels with second order slip boundary conditions and the requirement for development length," *eprint arXiv:1707.04947*, pp. 1-28, (2017).

[10] K. B. Patel, "Simulation of incompressible cylindrical duct flow with electrically conducting fluid using finite difference method," *Advances in Computational Sciences and Technology*, Vol. 10, No. 6, pp. 1663-1674, (2017).

[11] M. Sahu, P. Singh, S. S. Mahapatra, and K. K. Khatua, "Prediction of entrance length for low Reynolds number flow in pipe using neuro-fuzzy inference system," *Expert Systems with Applications*, Vol. 39, No. 4, pp. 4545-4557, (2012).

[12] S. Ray, B. Ünsal, and F. Durst, "Development length of sinusoidally pulsating laminar pipe flows in moderate and high Reynolds number regimes," *International Journal of Heat and Fluid Flow*, Vol. 37, pp. 167-176, (2012).

[13] M. Ö. Çarpınlıoğlu and E. Özahi, "Laminar flow control via utilization of pipe entrance inserts (a comment on entrance length concept)," *Flow Measurement and Instrumentation*, Vol. 22, No. 3, pp. 165-174, (2011).

[14] R. J. Poole and B. S. Ridley, "Development-length requirements for fully developed laminar pipe flow of inelastic non-Newtonian liquids," *Journal of Fluids Engineering*, Vol. 129, No. 10, pp. 1281-1287, (2007).

[15] C. Courtessole, S. Smolentsev, T. Sketchley, and M. Abdou, "MHD PbLi experiments in MaPLE loop at UCLA," *Fusion Engineering and Design*, Vol. 109-111, pp. 1016-1021, (2016).

[16] D. Wen and Y. Ding, "Experimental investigation into convective heat transfer of nanofluids at the entrance region under laminar flow conditions," *International Journal of Heat and Mass Transfer*, Vol. 47, No. 24, pp. 5181-5188, (2004).

[17] M. H. Taheri, M. Abbasi, and M. Khaki Jamei, "An integral method for the boundary layer of MHD non-Newtonian power-law fluid in the entrance region of channels," *Journal of the Brazilian Society of Mechanical Sciences and Engineering*, Vol. 39, No. 10, pp. 4177-4189, (2017).

[18] J. A. Shercliff, "Magnetohydrodynamic pipe flow Part2. High Hartmann number," *Journal of Fluid Mechanics*, Vol. 13, No. 4, pp. 513-518, (2006).

[19] S. K. A. Samad, "The flow of conducting fluids through circular pipes having finite conductivity and finite thickness under uniform transverse magnetic fields," *International Journal of Engineering Science*, Vol. 19, No. 9, pp. 1221-1232, (1981).

[20] X. Zhang, C. Pan, and Z. Xu, "Numerical analysis of liquid metal MHD flows through circular pipes based on a fully developed modeling," *Fusion Engineering and Design*, Vol. 88, No. 4, pp. 226-232, (2013).

[21] D. Krasnov, O. Zikanov, and T. Boeck, "Numerical study of magnetohydrodynamic duct flow at high Reynolds and Hartmann numbers," *Journal of Fluid Mechanics*, Vol. 704, pp. 421-446, (2012).

[22] S. Vantieghem, X. Albets-Chico, and B. Knaepen, "The velocity profile of laminar MHD flows in circular conducting pipes," *Theoretical and Computational Fluid Dynamics*, Vol. 23, p. 525, (2009).

[23] X. He and D. N. Ku, "Unsteady entrance flow development in a straight tube," *Journal of Biomechanical Engineering*, Vol. 116, No. 3, pp. 355-360, (1994).

[24] F. C. Li, T. Kunugi, and A. Serizawa, "MHD effect on flow structures and heat transfer characteristics of liquid metal–gas annular flow in a vertical pipe," *International Journal of Heat and Mass Transfer*, Vol. 48, No. 12, pp. 2571-2581, (2005).

[25] F. Durst, S. Ray, B. Ünsal, and O. A. Bayoumi, "The development lengths of laminar pipe and channel flows," *Journal of Fluids Engineering*, Vol. 127, No. 6, pp. 1154-1160, (2005).

[26] A. Malekzadeh, A. Heydarinasab, and B. Dabir, "Magnetic field effect on fluid flow characteristics in a pipe for laminar flow," *Journal of Mechanical Science and Technology*, Vol. 25, p. 333, (2011).

[27] Y. Li and O. Zikanov, "Laminar pipe flow at the entrance into transverse magnetic field," *Fusion Engineering and Design*, Vol. 88, No. 4, pp. 195-201, (2013).

[28] F. C. Li, D. Sutevski, S. Smolentsev, and M. Abdou, "Experimental and numerical studies of pressure drop in PbLi flows in a circular duct under non-uniform transverse magnetic field," *Fusion Engineering and Design*, Vol. 88, No. 11, pp. 3060-3071, (2013).

[29] L. Bühler and C. Mistrangelo, "Pressure drop and velocity changes in MHD pipe flows due to a local interruption of the insulation," *Fusion Engineering and Design*, Vol. 127, pp. 185-191, (2018).

[30] M. Javanmard, M. H. Taheri, and S. M. Ebrahimi, "Heat transfer of third-grade fluid flow in a pipe under an externally applied magnetic field with convection on wall," *Applied Rheology*, Vol. 28, No. 5, (2018).

[31] K. S. Arjun and R. Kumar, "Heat transfer in MHD square duct flow of nanofluid with discrete heat sources," *Transp Phenom Nano Micro Scales*, Vol. 6, No. 2, pp. 88-95, (2018).

[32] K. S. Arjun and R. Kumar, "Performance index in MHD duct nanofluid flow past a bluff body at high Re," *Journal of Mechanical Engineering*, Vol. 63, No. 4, pp. 235-247, (2017).

[33] K. S. Arjun and R. Kumar, "LBM analysis of micro-convection in MHD nanofluid flow," *Journal of Mechanical Engineering*, Vol. 63, No. 7-8, pp. 426-438, (2017).

[34] K. Arjun and K. Rakesh, "MHD and heat transfer analysis of nanofluid flow past a vertical porous plate," *Journal of Mechanical Engineering Research and Developments*, Vol. 40, No. 4, pp. 650-659, (2017).

[35] K. Arjun and K. Rakesh, "MHD natural convection heat transfer in a nanofluid filled finned square cavity," *Journal of Mechanical Engineering Research & Developments*, Vol. 40, pp. 481-489, (2017).

[36] P. A. Davidson, *An Introduction to Magnetohydrodynamics*. 1st ed., Cambridge University Press, (2001).

[37] S. Smolentsev, R. Moreau, and M. Abdou, "Characterization of key magneto-

hydrodynamic phenomena in PbLi flows for the US DCLL blanket," *Fusion Engineering and Design*, Vol. 83, No. 5-6, pp. 771-783, (2008).

[38] H. Madarame and H. Tokoh, "Development of computer code for analyzing liquid metal MHD flow in fusion reactor blankets, (II)," *Journal of Nuclear Science and Technology*, Vol. 25, No. 4, pp. 323-332, (1988).

[39] H. Madarame and H. Tokoh, "Development of computer code for analyzing liquid metal MHD flow in fusion reactor blankets, (I)," *Journal of Nuclear Science and Technology*, Vol. 25, No. 3, pp. 233-244, (1988).

[40] V. Sobolev, "Thermophysical properties of lead and lead-bismuth eutectic," *Journal of Nuclear Materials*, Vol. 362, No. 2-3, pp. 235-247, (2007).

[41] A. K. Mohanty and S. B. L. Asthana, "Compressible laminar flow in the inlet region of a smooth circular pipe," *Journal of Physics D: Applied Physics*, Vol. 13, No. 11, p. 2021, (1980).

How to cite this paper:

Mohammad Hasan Taheri, Morteza Abbasi and Mehran Khaki Jamei, "Development length of laminar magnetohydrodynamics pipe flows", *Journal of Computational and Applied Research in Mechanical Engineering*, Vol. 9, No. 2, pp. 397-407, (2019).

DOI: 10.22061/jcarme.2019.4416.1533

URL: http://jcarme.sru.ac.ir/?_action=showPDF&article=1020